https://doi.org/10.5194/egusphere-2022-665
Preprint. Discussion started: 11 October 2022

The Wetland Intrinsic Potential tool: Mapping wetland intrinsic potential through machine learning of multi-scale remote sensing proxies of wetland indicators

Meghan Halabisky [1], Dan Miller [2], Anthony J. Stewart [1], Daniel Lorigan [2], Tate Brasel [2] and L. Monika Moskal [1]

[1] School of Environmental and Forest Sciences, University of Washington, Seattle, WA, USA
[2] Terrainworks, Seattle, WA, USA;

Correspondence to: Meghan Halabisky (halabisk@uw.edu)

Abstract

Accurate, un-biased wetland inventories are critical to monitor and protect wetlands from future harm or land conversion. However, most wetland inventories are constructed through manual image interpretation or automated classification of multi-band imagery and are biased towards wetlands that are easy to detect directly in aerial and satellite imagery. Wetlands that are obscured by forest canopy, occur ephemerally, and those without visible standing water are, therefore, often missing from wetland maps. To aid in detection of these cryptic wetlands, we developed the Wetland Intrinsic Potential tool, based on a wetland indicator framework commonly used on the ground to detect wetlands through the presence of hydrophytic vegetation, hydrology, and hydric soils. Our tool uses a random forest model with spatially explicit input variables that represent all three wetland indicators, including novel multi-scale topographic indicators that represent the processes that drive wetland formation, to derive a map of wetland probability. With the ability to include multi-scale topographic indicators, the WIP tool can identify areas conducive to wetland formation and provides a flexible approach that can be adapted to diverse landscapes. For a study area in the Hoh River Basin in Western Washington, USA, classification of the output probability with a threshold of 0.5 provided an overall accuracy of 91.97%. Compared to the National Wetland Inventory, the classified WIP-tool output increased areas classified as wetland by 160% and reduced errors of omission from 47.5% to 14.1%, but increased errors of commission from 1.9% to 10.5%. The WIP tool is implemented using a combination of R and python scripts in ArcGIS.

Key Words: lidar, aerial imagery, soil moisture, forested wetlands

1 Introduction

Wetlands provide a vast array of ecosystem services, including water storage, carbon sequestration, sediment removal, and wildlife habitat (Davidson et al., 2019). Despite their value, over 50% of wetlands worldwide have been lost through draining and filling (Davidson, 2014; Davidson and Finlayson, 2018). Remaining wetlands are surrounded by an increasingly modified landscape that can adversely affect both the condition and function of wetlands (Calhoun et al., 2017; Tiner, 2009). An accurate inventory of wetland locations is necessary to protect wetlands from further landcover changes and degradation. However, in

https://doi.org/10.5194/egusphere-2022-665
Preprint. Discussion started: 11 October 2022

many regions, wetland inventories do not exist or are inaccurate with high errors of omission (Halabisky, 2019). Wetlands under partial or closed canopy, ephemeral wetlands that are flooded for only a portion of the year, and wetlands with no visible standing water (i.e. saturated soils) are often missing from wetland inventories (Halabisky, 2019).

On the ground, wetlands are identified by the presence of three wetland indicators; hydrophytic vegetation, surface hydrology (e.g., inundation or signs of inundation), and hydric soils (Cowardin, 1979). However, at the landscape scale, wetland inventories are commonly created through manual image interpretation by directly identifying wetland characteristics in imagery (e.g., presence of water) or proxies that represent wetland characteristics (e.g., areas of low slope represent areas more likely to be flooded) (Brinson, 1993; Tiner, 1990). In the last decade, there have been great strides in mapping wetlands through automated or semi-automated processes using remote sensing (Dronova, 2015; Halabisky, 2019; Kloiber et al., 2015; Lang and McCarty, 2009). Many of these methods rely in part or in total on the use of spectral imagery to detect wetlands. However, identification of wetlands under forest canopy or vegetation, ephemeral wetlands, and wetlands without visible standing water remains challenging.

Small, ephemeral wetlands with dense canopy cover are virtually undetectable in aerial imagery (Figure 1). Even in areas without dense canopy, trees and topography can create shadows in the imagery that can resemble flooded wetlands and confuse automated methods based on spectral features alone. Wetlands with fluctuating water levels or wetlands without visible surface water expression may not be easily detected in the imagery due to a mismatch in the image acquisition timing or poor spectral or spatial image resolution. These cryptic, undetected wetlands can comprise a substantial portion of total wetland area in certain landscapes (Creed et al., 2003; Janisch et al., 2011).

1.1 Topographic and hydrologic indices

Cryptic wetlands can be indirectly identified by mapping the hydrologic processes driving wetland inundation patterns. Many studies have shown that delineation of terrain attributes indicative of these processes is effective at predicting wetland locations (Lang et al., 2013; Maxwell et al., 2016; O'Neil et al., 2018), particularly when these attributes are calculated using high-resolution lidar elevation data. The primary attributes explored in the literature include local topographic position, slope gradient and curvature, the topographic wetness index, and the cartographic depth to water (Maxwell et al., 2018). These attributes are calculated using Digital Elevation Models (DEMs), which provide point measures of elevation over a regular grid.

Local topographic position provides a measure of vertical position in the landscape and can differentiate between higher and the low-lying terrain where wetlands tend to occur. There are a variety of methods to calculate local topographic position (Newman et al., 2018), all of which involve comparison of the elevation of a DEM grid point to the elevations of all the other

https://doi.org/10.5194/egusphere-2022-665
Preprint. Discussion started: 11 October 2022

grid points within a neighborhood of specified radius. The variety of methods for local topographic position differ in how these comparisons are made. The center-cell elevation can be compared to the minimum and maximum elevations or to the mean elevation. That elevation difference can then be used directly or normalized by the range of elevations, by the mean, or by the standard deviation. For mapping wetland potential, measures of local topographic position are used for identifying landforms where water may tend to accumulate (Branton and Robinson, 2020; Riley et al., 2017).

Slope gradient and curvature are related to the direction and rate of surface and shallow subsurface water flow across the terrain. Water tends to drain quickly from steep slopes and less quickly from lower-gradient slopes. Curvature can indicate areas where flow directions converge and where rates of flow decrease, both of which are associated with zones of increased soil moisture (Fink and Drohan, 2016).

The topographic wetness index is based on a simple conceptual model of shallow subsurface flow (e.g., Beven and Kirkby, 1979). The depth of soil saturation at a point, or at a DEM cell, is determined by the amount of water flowing to that cell, the degree of convergence or divergence of the topography there, and the effective velocity (the Darcy velocity) of saturated flow through the soil. Under steady-state rainfall, the amount of water is proportional to the area of the flow tube draining to that DEM cell. The effect of topographic convergence is accounted for by dividing that contributing area by the width of a contour line crossed by water flowing through the cell, giving the specific contributing area A_S. The flow velocity is proportional to the tangent of the slope θ. With these definitions, saturation depth varies with $A_s / \tan\theta$. The topographic wetness index is defined as TWI = $\ln(A_s / \tan\theta)$. TWI, also called the Compound Topographic Index (CTI), is used as a topographic indicator of relative soil moisture (Kopecký et al., 2021).

The cartographic depth to water (DTW) provides an estimated depth from the ground surface to the saturated zone in the soil column (Murphy et al., 2007). DTW calculates the elevation difference between a DEM grid point and a nearby location of water at the ground surface, such as a river or lake, which are included as inputs in the model. The location of the associated surface-water point is found by repeatedly finding the adjacent DEM cell with the smallest downslope elevation difference, jumping to that point, and repeating that procedure until surface water is encountered; that is, the least-cost path using slope as the measure of cost. Small DTW values can be good indicators of wetland occurrence (White et al., 2012). Height above the nearest drainage (Nobre et al., 2011) offers an alternative method for estimating depth to the saturated zone. This method finds the elevation difference between a DEM cell and the surface-water point it drains to based on the downslope flow path traced from each DEM cell (Rennó et al., 2008).

These terrain attributes in various combinations have all been used for wetland identification. The degree of success and the attributes of primary importance vary across studies. This variability reflects intrinsic differences across landscapes (Branton and Robinson, 2019), but also differences in the spatial resolution of the data used (Fink and Drohan, 2016), preconditioning

https://doi.org/10.5194/egusphere-2022-665
Preprint. Discussion started: 11 October 2022

of that data (O'Neil et al., 2018), and the specific topographic attributes examined. Another source of variability are differences in the spatial scale of the terrain attributes examined.

1.2 Multi-scale indices for complex topographic features

All of the terrain measures outlined above are dependent on the length scales over which measurements are calculated. For example, the local topographic position will vary depending on the neighborhood radius used (De Reu et al., 2013). A neighborhood spanning 20 meters will differentiate tree-fall pits and mounds (if resolved by the DEM) while a neighborhood radius spanning kilometers will differentiate valley floors and ridge tops. Gradient and curvature measured over 5 meters length might also detect pits and mounds while a gradient and curvature measured over 50 meters cannot, but can detect a broad swale. With measurement of any topographic attribute, it is important to match the scales of the landforms we wish to detect and of the processes we wish to characterize.

In regions with complex topography, wetlands are found in topographic features that occur at multiple, interconnected scales (Bertassello et al., 2018; Wu and Lane, 2017). These scales and the degree of interconnectedness vary across and within landscapes, depending on the landforms and hydrologic processes involved with wetland formation. This variability challenges our ability to use topographic attributes as general indicators of wetland potential. Is a 50-meter-wide depression as important as a 300-meter-wide depression, or a 1000-meter-wide depression? Does it matter if that 50-meter depression is inside of a 1000-meter depression? Likewise, does a depression on a valley floor have the same importance as a depression on a ridge top? Do the relevant scales differ across landscapes? To answer such questions, we must examine topographic attributes over multiple spatial scales.

There are a large range of factors to consider for wetlands detection: multispectral imagery, multiple interacting topographic attributes over a range of spatial scales, as well as datasets indicating variations in substrate, for example, differentiating terrain underlain by ice-sheet deposits from terrain underlain by bedrock. Analysis of such large and diverse datasets has benefited from the development of machine-learning algorithms that do not require assumptions about the statistical distribution of input data (Maxwell et al., 2018). Non-parametric supervised classification approaches to land cover mapping produce more efficient and accurate results than earlier supervised parametric classification methods (e.g. maximum likelihood) primarily because satellite image data values are not normally distributed (Wulder et al., 2019). Random forest modelling is a commonly used non-parametric classification method (Breiman, 2001), which allows for the use of multiple, correlated input variables that are not normally distributed. These methods are increasingly being used for remote detection of wetlands (Halabisky et al., 2018; Kloiber et al., 2015; Maxwell et al., 2016; O'Neil et al., 2018).

https://doi.org/10.5194/egusphere-2022-665
Preprint. Discussion started: 11 October 2022

1.3 Research Goal

Our goal was to develop a machine learning method using spatially explicit proxies for three wetland indicators: hydrophytic vegetation, hydrology, and hydric soils. We used this wetland indicator framework as an approach to ensure comprehensive inclusion of wetland characteristics in our model that reflects common wetland identification practices used by wetland ecologists. We developed and tested our model in the Hoh River watershed of Northwest Washington State, a particularly challenging area to map due to its complex topography, tall and structurally complex forests, and high variability of wetland types, including many ephemeral wetlands under dense canopy. We used the methods outlined here to create a flexible ArcGIS tool called the Wetland Intrinsic Potential (WIP) Tool that provides an end-to-end workflow that enables users to develop proxies for wetland indicators, include a wide range of topographic indices at multiple scales, and run a random forest model to create predicted wetland inventories for their area of interest.

2 Study area and datasets

Here we define wetlands broadly as wet areas that have one of three wetland indicators; hydric vegetation, hydric soils, or signs of inundation for at least two weeks during the growing season. We included both ephemeral and permanent waterbodies such as rivers and streams in our wetland definition. This decision was driven by the National Wetland Inventory which includes open water features, such as lakes and rivers (Cowardin, 1979).

2.1 Study area

Data collection and model evaluation were performed in the Hoh watershed on the Pacific Northwest coast of Washington State, USA (Figure 1). The Hoh watershed contains a broad valley filled with alluvial and alpine glacial deposits, with steep alpine zones predominately in marine sedimentary rocks. The Hoh is part of the Olympic temperate rainforest, receiving on average between 2.8 and 4.3 meters of precipitation a year, based on PRISM 30-year normals (https://prism.oregonstate.edu/normals/). While the lower watershed has undergone significant impacts from forest harvest, the upper watershed is part of the Olympic National Park (ONP) where forest harvest is prohibited. The trees of the old-growth forest in the ONP can be up to 80 m in height (Harmon and Franklin, 1989) while the lower watershed is dominated plantation forests managed for timber harvest (Pelt, 2001). The wetlands within the Hoh watershed are diverse, from precipitation-driven peat bogs to riparian wetlands driven by stream flow inputs as well as wetlands driven by surface water flows and groundwater inputs. Many of the wetlands are under completely closed canopy cover; however, many of the trees in areas of high levels of inundation display stunted growth. The main river channel is active and unconfined and has formed terraces from previous higher flows.

https://doi.org/10.5194/egusphere-2022-665
Preprint. Discussion started: 11 October 2022

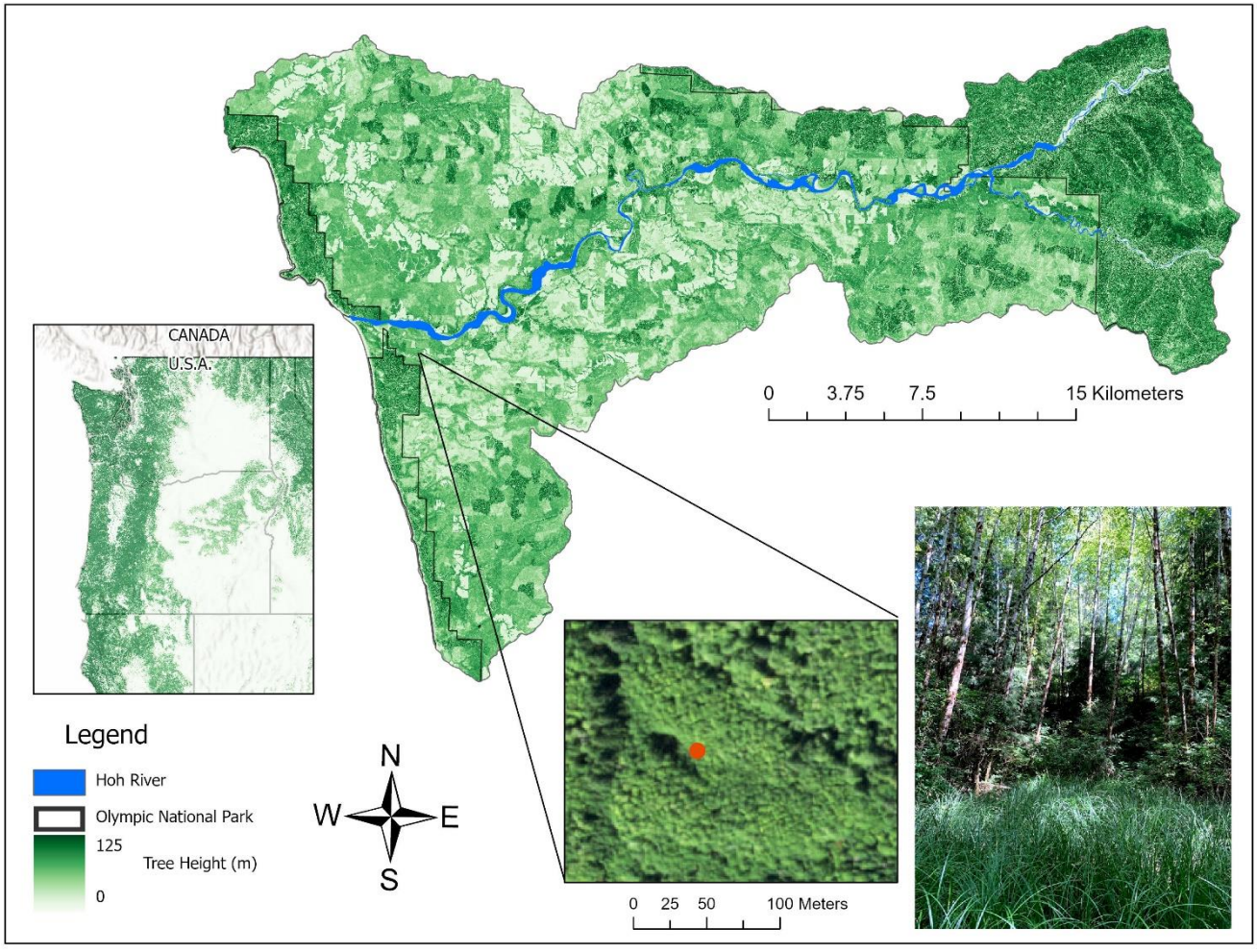

Figure 1. Study area in the Hoh rainforest located in the Pacific Northwest of the United States. Study area shows the variability in tree height largely determined by a legacy of forestry. Areas within Olympic National Park have not been logged. The photo on the right is a picture taken on the ground of the forested wetland shown in the aerial image from the 2017 National Aerial Imagery Program (NAIP) (orange dot). This wetland was missed in the National Wetland Inventory and is hard to detect in the aerial imagery. The dark areas in the aerial image are created by shadows from trees and are not standing water.

2.2 Data sources

We used multiple raster and vector datasets as inputs and training data into our random forest model:

1. 4-band aerial imagery acquired by the National Aerial Imagery Program (NAIP) in 2017 at 1m resolution.
2. A DEM and digital surface model (DSM) derived from lidar acquired in 2012 and 2013 by Watershed Sciences at 3-foot pixel resolution and downloaded from the Washington State Department of Natural Resources Lidar data portal

https://doi.org/10.5194/egusphere-2022-665
Preprint. Discussion started: 11 October 2022

(https://lidarportal.dnr.wa.gov/). A DSM is a surface model created from the highest hit object in the lidar point cloud. Subtracting the DEM from the DSM provides estimates of canopy height.

3. Two data layers from the SSURGO soils data for the Hoh watershed: the depth to any restricted layer and the hydraulic conductivity.

We used the National Wetland Inventory to create an initial sample training dataset for our preliminary model. Before processing, we re-scaled all of the raster input datasets to match a 4m pixel resolution. The reason for re-scaling to a coarser pixel resolution was to reduce processing time, while still preserving the resolution needed for wetland identification.

3 Methods

3.1 Developing proxies for wetland indicators

As a first step, we identified spatially explicit proxies that represent wetland indicators for hydrophytic vegetation, hydrology, and hydric soils that we could either derive from aerial imagery, lidar data, or are freely available (i.e., SSURGO soils) (Figure 2). This framework provided us with a systematic way to consider the characteristics used to identify wetlands in the field and in imagery and determine the ideal proxy that could represent these characteristics as inputs in a random forest model. This framework also allowed us a way to test which group of indicators was most useful in identifying wetlands. We identified datasets that represented proxies based on our own experience and from a thorough literature review.

https://doi.org/10.5194/egusphere-2022-665
Preprint. Discussion started: 11 October 2022

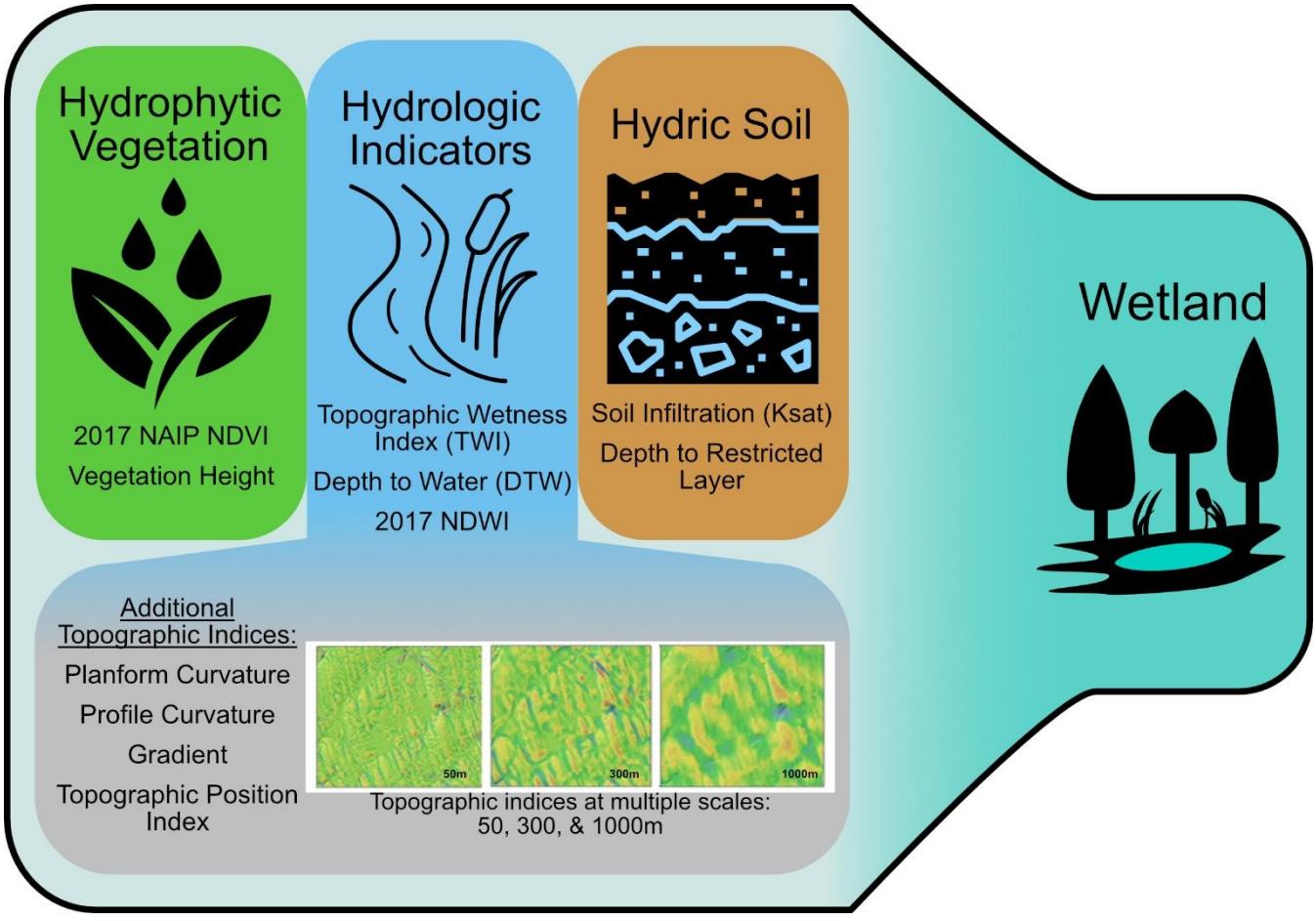

Figure 2. Input variables used in the random forest model represent proxies of wetland indicators used for wetland identification. Topographic indices, calculated at multiple scales, represent areas where water flows and collects. Profile curvature calculated at three different scales; 50m, 300m, & 1000m scale is shown as an example.

3.1.1 Hydrologic Indicators

We identified surface water directly in the imagery using the normalized difference water index (NDWI) created from the 2017 NAIP imagery. The NDWI is a normalized band ratio between the near infrared and green bands that is useful to identify open water (McFeeters, 1996). We generated the TWI and the DTW indices using the ArcHydro toolbox in ArcPro using permanent riverine features and waterbodies in the National Hydrography Dataset as input water features for DTW (O'Neil et al., 2018).

In addition to the TWI and the DTW, we explored the use of topographic indices calculated at different length scales.

https://doi.org/10.5194/egusphere-2022-665
Preprint. Discussion started: 11 October 2022

Gradient and curvature were calculated using the methodology described by Zevenbergen and Thorne, (1987) in which the shape of the ground surface at a DEM grid point is interpolated as a smooth polynomial surface that matches elevations of the grid point and its eight adjacent points. This methodology was modified to use a circular neighbourhood (Shi et al., 2007) of arbitrary radius, with elevations along the circle interpolated from adjacent DEM grid points. This procedure allows estimates of gradient and curvature for each DEM point measured over any length scale, down to the DEM grid size. As a measure of local relief, we used deviation from mean elevation (DEV). $DEV = (z\text{-}z_{mean})/\sigma$, where z is elevation at the point of measurement, z_{mean} is the mean elevation within a neighborhood of specified radius, and σ is the standard deviation of elevation within that neighbourhood (Newman et al., 2018). Positive values of DEV indicate the point is higher than the mean of neighboring points (within the specified radius); negative values indicate the point is lower. Dividing by the standard deviation – a measure of how variable elevations are within the neighborhood – acts to normalize DEV values so that depressions in gentle, low-relief terrain, like broad river valleys, are recognized just as well as depressions in high-relief terrain, like alpine glacial cirques.

We calculated the topographic indices at five different length scales, 50m, 150m, 300m, 500m, 1000m to approximate the variability of topographic features across the landscape. We visually assessed each topographic index at these scales and decided to only use scales 50m, 300m, and 1000m as they captured the most variability across the landscape and to reduce the number of input datasets to improve processing time.

Topographic indices were calculated using compiled Fortan programs from the Netstream program suite (Miller, 2003). These programs implement the procedures described above for calculating gradient, curvature, and local relief over any length scale. We developed an ArcGIS Pro toolbox called DEM Utilities for users to create topographic indices at multiple scales.

3.1.2 Hydrophytic vegetation and hydric soil indicators

To detect hydric vegetation, we created a normalized difference vegetation index (NDVI) from the 2017 NAIP imagery for 2017, rescaled to 4 meters. NDVI is a normalized band ratio between the near infrared and red bands that is useful at distinguishing wetland from non-wetland vegetation, as well as vegetation that may be stressed from inundation (Halabisky, 2011). We created two raster datasets from the SSURGO soil database, depth to any restricted layer and the hydraulic conductivity, to differentiate the soil properties that influence soil saturation and drainage.

3.2 Training Data

Without knowing the location of forested wetlands a priori, it was difficult to develop an efficient and unbiased sampling design. Therefore, to aid in placement of points for a training dataset, we used a stratified random sample from a preliminary wetland model developed from the National Wetland Inventory (NWI, https://www.fws.gov/program/national-wetlands-

https://doi.org/10.5194/egusphere-2022-665
Preprint. Discussion started: 11 October 2022

inventory) for the Hoh watershed. The preliminary model was based on a random forest model using the topographic indices and trained on 1000 wetland and 2000 non-wetland locations sampled from the NWI. The preliminary model then consisted of a raster of wetland probability with values from 0 to 1. To generate point locations for training the final model, we randomly placed 600 sample points equally into four strata based on the preliminary wetland probability raster: 0 – 0.25, 0.25 – 0.5, 0.5 – 0.75, 0.75 – 1.0. This provided an efficient way to identify potential wetland (high probability) and non-wetland (low probability) areas for a balanced point placement, as well as areas where there is high model uncertainty (i.e., probability near 0.5). We felt that stratifying the sample points using the preliminary model would reduce potential bias introduced by referencing the NWI better than if we had solely used the NWI to create our sample stratification.

Each sample point was evaluated by two analysts and labelled as wetland or upland using available datasets, including a hillshade and slope index from the lidar DEM, pre-existing wetland inventories including the NWI, NAIP imagery, and Forest Practices permits issued by the Washington State Department of Natural Resources, which indicate the presence of wetlands in areas where timber harvest occurs. If a point could not be determined as a wetland or non-wetland in aerial imagery or any other available datasets, it was marked as unknown. The challenge with this approach is that many of the areas with model certainty close to 0.5 are hard to assess using image interpretation. We made several site visits to ensure that assumptions made in manual image interpretation aligned with the ground truth. In 25 cases where the edge of the wetland was difficult to determine, the point was moved to an area clearly inside or outside the wetland. We removed 2 points because we could not agree on the label. We were unable to identify any wetlands formed by groundwater expression on slopes with no channel formation to include in the training or validation dataset. Therefore, we expected that the model could not predict or validate the presence of these type of slope wetlands.

3.3 Random Forest Model

We used the randomForest package in R (Breiman, 2001) with 598 sample points and 200 trees to train random forest models using 19 wetland indicators (Figure 2). We decided to use the most complete model with all 19 input data layers based on comparison of the out-of-bag error, a bootstrapped validation approach using sub-selections of the training data. The final model provided a raster showing the probability that a wetland will be found at each DEM grid cell (Figure 3). The Gini coefficient provides a measure of the relative importance of each input indicator in the final model (Figure 4). We classified the wetland probability values into a binary classification of upland and wetland classes using a probability threshold of 0.5.

3.4 Model Validation

To validate the WIP model, we created a wetland classification from all pixels with a probability score of 0.5 or above. We used this classification to randomly distribute 100 points within the wetland area and 200 points in the area outside the wetland classification (i.e. upland). We used the same two-person image interpretation process used for the training sample to label the 300 points. We moved 5 points because we could not detect the wetland edge and removed one point because the analysts

https://doi.org/10.5194/egusphere-2022-665
Preprint. Discussion started: 11 October 2022

could not agree on a label. We used the validation dataset to assess the accuracy of the random forest output and to identify errors of omission and commission.

4 Results

Our WIP model for the Hoh watershed predicting wetland locations had an overall accuracy of 91.97% when using a threshold probability of 0.5. The wetland error of commission (false positives) was 10.53% and the error of omission (false negatives, missed wetlands) was 14.14%. In contrast, the current NWI for the Hoh watershed had an overall accuracy of 83.95%, with an error of commission of 1.89% and an error of omission of 47.47%.

Table 1. Accuracy assessment for WIP model

		Reference Data			
		Wetland	Upland	Total	Commission error
Model Results	Wetland	85	10	95	10.53%
	Upland	14	190	204	6.86%
	Total	99	200		
	Omission error	14.14%	5.00%	Overall Accuracy = 275/299 (91.97%)	

Our WIP model for the Hoh mapped 6,995 hectares of wetlands, a 160% increase in the area of wetlands mapped by the NWI. Gradient calculated at a scale of 50m, tree height (derived from lidar), and local elevation with a scale of 300m were identified as the three variables that contributed the most importance to the model as measured by the Gini importance (Figure 4). Amongst categories shown in Figure 2., there were slightly more topographic indices loading strongly as predictors. Less significant metrics included the coarser 1000m length scales of topography indices, with the exception of the 1000m gradient metric. Other lower metrics included the depth to the restrictive layer and the TWI.

https://doi.org/10.5194/egusphere-2022-665
Preprint. Discussion started: 11 October 2022

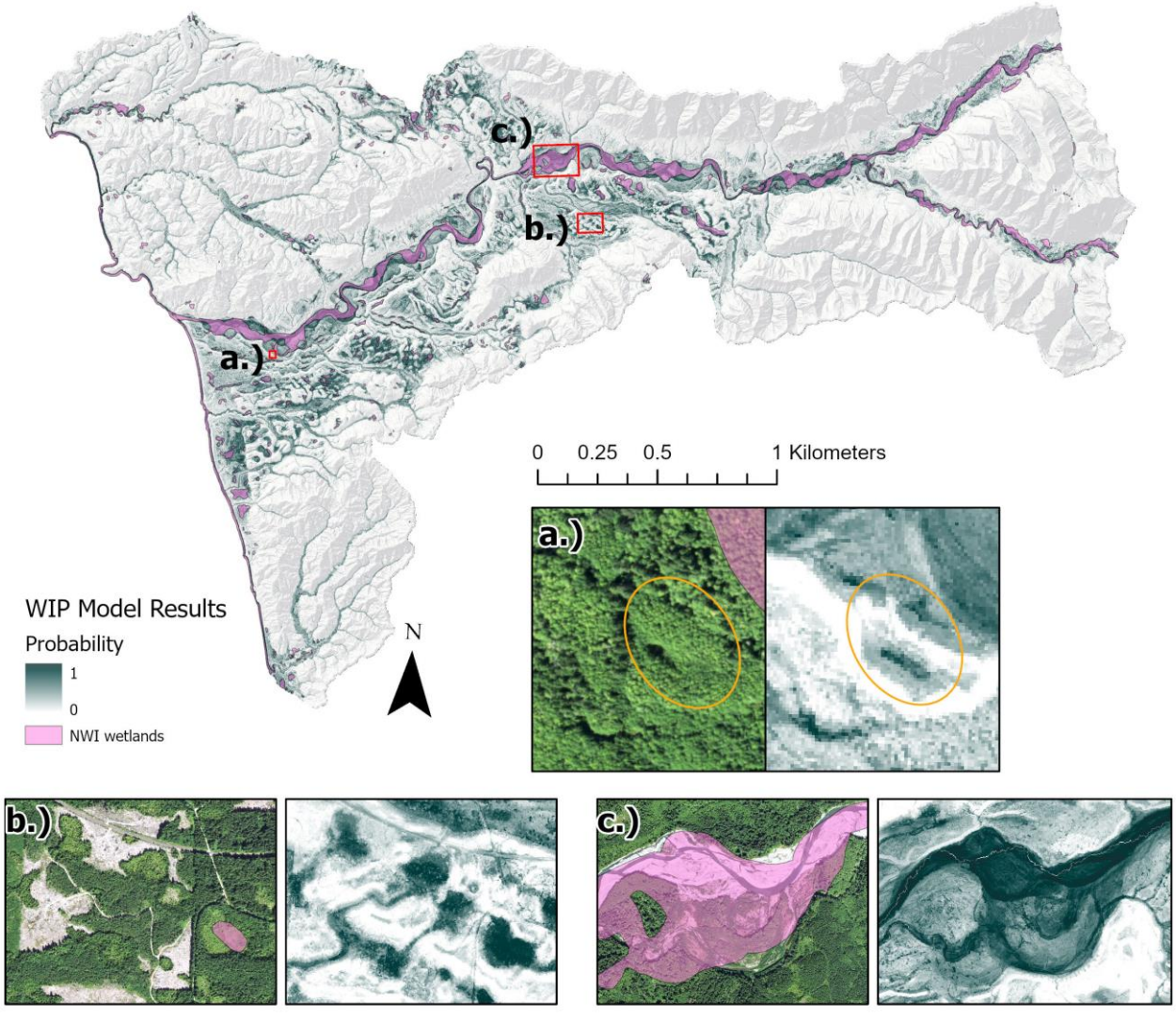

Figure 3. Wetland probability map of the entire study area with three examples: Depressional wetland (a.), peatland (b.), and riverine wetland (c.).

285

Of the 14 labelled wetland points misclassified in the WIP model as upland (errors of omission), nine of them were within 5 meters of the WIP wetland classification. Conversely, none of the 50 labelled wetland points misclassified as upland (errors of omission) in the NWI model were within 5 meters of the NWI.

https://doi.org/10.5194/egusphere-2022-665
Preprint. Discussion started: 11 October 2022

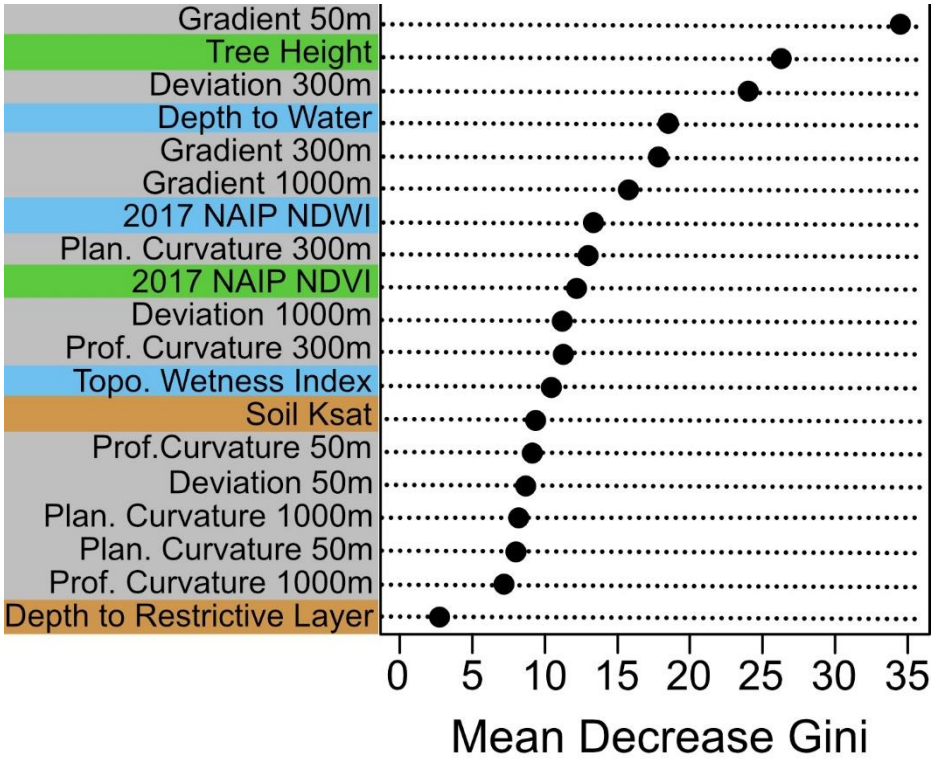

290

Figure 4. Gini coefficient output from the WIP tool random forest model, which is a measure of how each variable contributes to the homogeneity of the nodes and leaves in the resulting random forest. The variables at the top of the chart contributed the most to the model results.

5 Discussion

295 The Wetland Intrinsic Potential tool was designed to improve the detection of wetlands with a specific focus on increasing detection of cryptic wetlands obstructed by vegetation canopy, influenced by shadows from nearby objects and steep topography, and wetlands that do not have visible standing water for some part of the year. Using a WIP probability threshold of 0.5, we were able to identify wetlands that were missed in the existing NWI because of these challenging, yet common remote-sensing issues. Our model reduced the error of omission by over 33% and the overall accuracy increased by 8%
300 compared to the NWI. The increase in overall accuracy from the NWI was driven by the large reduction in errors of omission. It is important to keep in mind that the NWI has a minimum mapping unit of 0.5 ha, while our WIP tool did not set a minimum mapping and is only limited by the resolution of the input DEM.

https://doi.org/10.5194/egusphere-2022-665
Preprint. Discussion started: 11 October 2022

Our wetland indicator framework allowed us to comprehensively assess a full suite of variables for wetland identification, while providing a flexible approach that can be adapted to other areas with different topographic features and wetland types. For our study area, we found that a combination of proxies representing all three wetland indicators contributed to the overall model importance. However, indicators for hydrologic features and hydrophytic vegetation contributed the most. Specifically, three topographic indices that represent hydrologic features were among the top five input variables. It is unsurprising that measurements of gradient contributed the most, as wetlands are found primarily in areas of low slope. Tree height was the second contributing data layer, which may be driven by both the preference for timber companies to harvest outside of wetlands and the stunted height of trees in wetlands. We did notice that while including tree height improved our model, it also led to an increase in errors of commissions in harvested areas. Users who are interested in identifying wetlands in areas with timber harvest may choose not to include tree height to remove this bias. Measurements of DEV at a scale of 300 was also a top contributing factor, which is useful in identifying medium sized depressions. Proxies for hydric soils did not contribute as much to the model as other wetland indicator proxies. The hydrologic indicator DTW contributed more than the TWI.

5 .1 Model error

Systematic errors can provide clues for improving model performance. An exploration of the misclassified points shows that, for this study area, zones with the highest commission error are located around the main river channel. This suggests that large floodplain and terrace zones should be delineated as categorical variables for input to the random forest model. Several old river terraces in old-growth forest stands were also misclassified as wetlands. Further investigation of these points on the ground suggest that these areas are right on the edge of meeting the definition of a wetland.

Because the majority of the errors of omission were within 5m of a mapped wetland suggests that the model can identify wetland areas, but struggles to accurately delineate the wetland boundary. Some wetlands have clear boundaries, while others have a subtle wet-dry gradient. In these locations, the edges of wetlands can be hard to delineate on the ground. For wetland types without hard boundaries, the wetland probability output may provide more realistic information as it picks up the wet-dry gradient. Regardless, while the WIP tool can be useful to aid wetland delineations, standard field techniques on the ground are required for precise wetland delineation. We did not include slope wetlands in our study because of the difficulty of finding enough samples to train our model for this class of wetlands.

We used a threshold of 0.5 and above to classify wetlands for our accuracy assessment. If users want to lower errors of omission a lower threshold is recommended. Conversely, if users prefer to avoid over mapping, a higher threshold should be selected.

https://doi.org/10.5194/egusphere-2022-665
Preprint. Discussion started: 11 October 2022

5.2 Extension of model to new locations

Extension of the model to new areas requires new training data. The ability of a model to predict wetland occurrence depends on how well the data used to train the model represent the range of wetland types and locations that exist on the ground. Our intention was not to develop a model that could be extended to new areas without the collection of new training data. A model trained on one study area, but run on a different study area, will not produce accurate results if the two study areas are dissimilar. The importance of different wetland indicators can vary for different study areas, but often the variables themselves will vary in importance as well. For example, in one watershed that contains many surface-water driven wetlands, the topographic wetness index may be the most important variable that describes the variability between wetlands and uplands, but in another study area, DTW may be ranked as a more important contributing variable.

The WIP tool is designed to be both flexible and allow for iterative improvements from inclusion of additional datasets (e.g. Sentinel-1 data). While our goal here was to develop a model with high accuracy and assess multiple wetland indicator proxies, we also realize that our comprehensive approach may present hurdles to those in areas where some of the data inputs are unavailable. Here we developed a model to optimize for overall accuracy. However, a modified version of the WIP tool with fewer inputs can provide useful results, especially if the probability gradient does not need to be converted into a hard classification. In cases, where a hard wetland classification is not the goal, it may be justifiable to focus only on lidar-derived data inputs as a starting point and include spectral or soils data only if out-of-bag error is not adequate.

In this study area, we used a lidar-derived DEM to create our random forest model input datasets. While lidar data is becoming increasingly more widespread, it is not available everywhere. For areas without lidar coverage, the WIP tool can still be run with a DEM that was not created from a lidar acquisition. We have qualitatively tested out models using a 1/3-arc-second National Elevation Dataset DEM and an IfSAR-derived DEM and found them both to provide potentially adequate results, although at a coarser spatial resolution.

While we tested this model in a heavily forested area, we believe the WIP tool could be applied to identify wetlands in other landscapes, such as agricultural areas, rangelands, and non-forested areas. However, none of the variables we included in our testing captured water movement influenced by human activity, such as water infrastructure, draining, ditching, or damming. Therefore, we expect that in areas with high levels of human modification of the hydrology the WIP model may identify areas of intrinsic potential and not necessarily areas that meet current definitions of a wetland.

https://doi.org/10.5194/egusphere-2022-665
Preprint. Discussion started: 11 October 2022

5.3 Model availability

We designed the WIP tools for this project expecting that they will evolve over time. The scripts and software are licensed as open source and publicly available. The python and R scripts for the DEMutilities and Wetland Tool ArcGIS Pro toolboxes are posted to a public github repository at https://github.com/TerrainWorks-Seattle/ForestedWetlands. Bug reports, comments, and feature requests for these toolboxes can be submitted by posting an issue on github. The random forest model can readily accommodate new terrain attributes as explanatory variables and the scripts in the Wetland Tools toolbox can accommodate any input grid that can be imported to ArcGIS. We used the R-ArcGIS Bridge to build the Wetland Tools ArcGIS Pro toolbox that implement scripts that call R functions to build and apply random forest models.

6 Conclusion

Wetland inventories are critical sources of data to support wetland conservation prioritization, land use permitting and regulations, monitoring, and wetland research. While wetland features may individually be small, collectively they cover vast areas and contribute to critical ecosystem services. The omission of a large percentage of wetlands within a region impedes our understanding of the total ecosystem services provided by wetlands and how specific land use regulations and policies may impact these services.

Accurate, unbiased wetland inventories are necessary to avoid further degradation and losses of wetlands. The WIP tool was specifically developed to identify cryptic wetlands that are missing from existing wetland inventories, but can also be applied to areas where wetlands have not been mapped well. Our wetland indicator framework, which includes spatial variables representing hydrophytic vegetation, hydrology, and hydric soils, can be used to quantify probability of wetland occurrence, including cryptic wetlands, with high confidence. The inclusion of novel multi-scale topographic attributes greatly improved model results as they were able to capture the variability of topographic features conducive to wetland formation. Our wetland indicator framework provides a flexible approach that can be adapted to identify diverse wetland types across varied landscapes. We expect that the capabilities of the WIP tool will expand over time as users determine the most effective wetland indicators used for identifying wetlands in other regions.

https://doi.org/10.5194/egusphere-2022-665
Preprint. Discussion started: 11 October 2022

7 Code/Data availability

The Fortran programs used to build the raster data sets are licensed under the Gnu Public License[1], version 3. The python and R scripts for the DEMutilities and Wetland Tool ArcGIS Pro toolboxes are posted to a public github repository at https://github.com/TerrainWorks-Seattle/ForestedWetlands. TerrainWorks maintains all software developed during collaborative projects. Input data, training data, and outputs can be downloaded at

8 Author contribution

MH, DM, AJS, and LMM designed the sampling, methods, and model design and MH and AJS carried them out. MH, DM, TB, and DL developed the model code and MH performed the simulations. MH prepared the manuscript with contributions from all authors.

9 Competing interests

The authors declare that they have no conflict of interest.

10 Acknowledgements

The authors would like to acknowledge Vivian Griffey, Sage Ince, Astrid Sanna, Amy Yahnke, and the Washington State CMER Wetland Scientific Advisory group for support collecting training data out in the field. Initial development and testing of the WIP tool was funded by the CMER Wetland Scientific Advisory Group. Final model development was funded through the NASA Carbon Monitoring Science Program (Grant # 80NSSC20K0427).

10 References

Bertassello, L.E., Rao, P.S.C., Jawitz, J.W., Botter, G., Le, P.V.V., Kumar, P., Aubeneau, A.F., 2018. Wetlandscape Fractal Topography. Geophys. Res. Lett. 45, 6983–6991. https://doi.org/10.1029/2018GL079094

Branton, C., Robinson, D.T., 2020. Quantifying Topographic Characteristics of Wetlandscapes. Wetlands 40, 433–449. https://doi.org/10.1007/s13157-019-01187-2

Breiman, L., 2001. Random Forests. Mach. Learn. 45, 5–32. https://doi.org/10.1023/A:1010933404324

Brinson, M.M., 1993. A Hydrogeomorphic Classification for Wetlands (No. Technical Report WRP-DE-4). US Army Corps of Engineers, Waterways Experiment Station, Vicksburg, MS, USA.

Calhoun, A.J.K., Mushet, D.M., Bell, K.P., Boix, D., Fitzsimons, J.A., Isselin-Nondedeu, F., 2017. Temporary wetlands: challenges and solutions to conserving a 'disappearing' ecosystem. Biol. Conserv., Small Natural Features 211, 3–11. https://doi.org/10.1016/j.biocon.2016.11.024

Cowardin, L.M., 1979. Classification of Wetlands & Deepwater Habitats of the U. S. Diane Publishing Company.

[1] https://www.gnu.org/licenses/gpl-3.0.en.html

https://doi.org/10.5194/egusphere-2022-665
Preprint. Discussion started: 11 October 2022

Creed, I.F., Sanford, S.E., Beall, F.D., Molot, L.A., Dillon, P.J., 2003. Cryptic wetlands: integrating hidden wetlands in regression models of the export of dissolved organic carbon from forested landscapes. Hydrol. Process. 17, 3629–3648. https://doi.org/10.1002/hyp.1357

Davidson, N.C., 2014. How much wetland has the world lost? Long-term and recent trends in global wetland area. Mar. Freshw. Res. 65, 934. https://doi.org/10.1071/MF14173

Davidson, N.C., Dam, A.A. van, Finlayson, C.M., McInnes, R.J., Davidson, N.C., Dam, A.A. van, Finlayson, C.M., McInnes, R.J., 2019. Worth of wetlands: revised global monetary values of coastal and inland wetland ecosystem services. Mar. Freshw. Res. 70, 1189–1194. https://doi.org/10.1071/MF18391

Davidson, N.C., Finlayson, C.M., 2018. Extent, regional distribution and changes in area of different classes of wetland. Mar. Freshw. Res. 69, 1525. https://doi.org/10.1071/MF17377

De Reu, J., Bourgeois, J., Bats, M., Zwertvaegher, A., Gelorini, V., De Smedt, P., Chu, W., Antrop, M., De Maeyer, P., Finke, P., Van Meirvenne, M., Verniers, J., Crombé, P., 2013. Application of the topographic position index to heterogeneous landscapes. Geomorphology 186, 39–49. https://doi.org/10.1016/j.geomorph.2012.12.015

Dronova, I., 2015. Object-Based Image Analysis in Wetland Research: A Review. Remote Sens. 7, 6380–6413. https://doi.org/10.3390/rs70506380

Fink, C.M., Drohan, P.J., 2016. High Resolution Hydric Soil Mapping using LiDAR Digital Terrain Modeling. Soil Sci. Soc. Am. J. 80, 355–363. https://doi.org/10.2136/sssaj2015.07.0270

Halabisky, M., 2019. Improved wetland identification for conservation and regulatory priorities.

Halabisky, M., 2011. Object-based classification of semi-arid wetlands. J. Appl. Remote Sens. 5, 053511. https://doi.org/10.1117/1.3563569

Halabisky, M., Babcock, C., Moskal, L., 2018. Harnessing the Temporal Dimension to Improve Object-Based Image Analysis Classification of Wetlands. Remote Sens. 10, 1467. https://doi.org/10.3390/rs10091467

Harmon, M.E., Franklin, J.F., 1989. Tree Seedlings on Logs in *Picea-Tsuga* Forests of Oregon and Washington. Ecology 70, 48–59. https://doi.org/10.2307/1938411

Janisch, J.E., Foster, A.D., Ehinger, W.J., 2011. Characteristics of small headwater wetlands in second-growth forests of Washington, USA. For. Ecol. Manag. 261, 1265–1274. https://doi.org/10.1016/j.foreco.2011.01.005

Kloiber, S.M., Macleod, R.D., Smith, A.J., Knight, J.F., Huberty, B.J., 2015. A Semi-Automated, Multi-Source Data Fusion Update of a Wetland Inventory for East-Central Minnesota, USA. Wetlands 35, 335–348. https://doi.org/10.1007/s13157-014-0621-3

Kopecký, M., Macek, M., Wild, J., 2021. Topographic Wetness Index calculation guidelines based on measured soil moisture and plant species composition. Sci. Total Environ. 757, 143785. https://doi.org/10.1016/j.scitotenv.2020.143785

Lang, M., McCarty, G., Oesterling, R., Yeo, I.-Y., 2013. Topographic Metrics for Improved Mapping of Forested Wetlands. Wetlands 33, 141–155. https://doi.org/10.1007/s13157-012-0359-8

Lang, M.W., McCarty, G.W., 2009. Lidar intensity for improved detection of inundation below the forest canopy. Wetlands 29, 1166–1178. https://doi.org/10.1672/08-197.1

Maxwell, A.E., Warner, T.A., Fang, F., 2018. Implementation of machine-learning classification in remote sensing: an applied review. Int. J. Remote Sens. 39, 2784–2817. https://doi.org/10.1080/01431161.2018.1433343

Maxwell, A.E., Warner, T.A., Strager, M.P., 2016. Predicting Palustrine Wetland Probability Using Random Forest Machine Learning and Digital Elevation Data-Derived Terrain Variables. Photogramm. Eng. Remote Sens. 82, 437–447. https://doi.org/10.14358/PERS.82.6.437

McFeeters, S.K., 1996. The use of the Normalized Difference Water Index (NDWI) in the delineation of open water features. Int. J. Remote Sens. 17, 1425–1432. https://doi.org/10.1080/01431169608948714

Miller, D.J., 2003. Programs for DEM Analysis, Landscape Dynamics and Forest Mangement, General Technical Report RMRS-GTR-101CD.

Murphy, P.N.C., Ogilvie, J., Connor, K., Arp, P.A., 2007. Mapping wetlands: A comparison of two different approaches for New Brunswick, Canada. Wetlands 27, 846–854. https://doi.org/10.1672/0277-5212(2007)27[846:MWACOT]2.0.CO;2

Newman, D.R., Lindsay, J.B., Cockburn, J.M.H., 2018. Evaluating metrics of local topographic position for multiscale geomorphometric analysis. Geomorphology 312, 40–50. https://doi.org/10.1016/j.geomorph.2018.04.003

https://doi.org/10.5194/egusphere-2022-665
Preprint. Discussion started: 11 October 2022

Nobre, A.D., Cuartas, L.A., Hodnett, M., Rennó, C.D., Rodrigues, G., Silveira, A., Waterloo, M., Saleska, S., 2011. Height Above the Nearest Drainage – a hydrologically relevant new terrain model. J. Hydrol. 404, 13–29. https://doi.org/10.1016/j.jhydrol.2011.03.051

O'Neil, G.L., Goodall, J.L., Watson, L.T., 2018. Evaluating the potential for site-specific modification of LiDAR DEM derivatives to improve environmental planning-scale wetland identification using Random Forest classification. J. Hydrol. 559, 192–208. https://doi.org/10.1016/j.jhydrol.2018.02.009

Pelt, R.V., 2001. Forest Giants of the Pacific Coast. Global Forest Society.

Rennó, C.D., Nobre, A.D., Cuartas, L.A., Soares, J.V., Hodnett, M.G., Tomasella, J., Waterloo, M.J., 2008. HAND, a new terrain descriptor using SRTM-DEM: Mapping terra-firme rainforest environments in Amazonia. Remote Sens. Environ. 112, 3469–3481. https://doi.org/10.1016/j.rse.2008.03.018

Riley, J.W., Calhoun, D.L., Barichivich, W.J., Walls, S.C., 2017. Identifying Small Depressional Wetlands and Using a Topographic Position Index to Infer Hydroperiod Regimes for Pond-Breeding Amphibians. Wetlands 37, 325–338. https://doi.org/10.1007/s13157-016-0872-2

Shi, X., Zhu, A.-X., Burt, J., Choi, W., Wang, R., Pei, T., Li, B., Qin, C., 2007. An Experiment Using a Circular Neighborhood to Calculate Slope Gradient from a DEM. Photogramm. Eng. Remote Sens. 73, 143–154. https://doi.org/10.14358/PERS.73.2.143

Tiner, R.W., 2009. Global Distribution of Wetlands, in: Likens, G.E. (Ed.), Encyclopedia of Inland Waters. Academic Press, Oxford, pp. 526–530. https://doi.org/10.1016/B978-012370626-3.00068-5

Tiner, R.W., 1990. Use of high-altitude aerial photography for inventorying forested wetlands in the United States. For. Ecol. Manag. 33–34, 593–604. https://doi.org/10.1016/0378-1127(90)90221-V

White, B., Ogilvie, J., Campbell, D.M.H.M.H., Hiltz, D., Gauthier, B., Chisholm, H.K.H., Wen, H.K., Murphy, P.N.C.N.C., Arp, P.A.A., 2012. Using the Cartographic Depth-to-Water Index to Locate Small Streams and Associated Wet Areas across Landscapes. Can. Water Resour. J. Rev. Can. Ressour. Hydr. 37, 333–347. https://doi.org/10.4296/cwrj2011-909

Wu, Q., Lane, C.R., 2017. Delineating wetland catchments and modeling hydrologic connectivity using lidar data and aerial imagery. Hydrol. Earth Syst. Sci. 21, 3579–3595. https://doi.org/10.5194/hess-21-3579-2017

Wulder, M.A., Loveland, T.R., Roy, D.P., Crawford, C.J., Masek, J.G., Woodcock, C.E., Allen, R.G., Anderson, M.C., Belward, A.S., Cohen, W.B., Dwyer, J., Erb, A., Gao, F., Griffiths, P., Helder, D., Hermosilla, T., Hipple, J.D., Hostert, P., Hughes, M.J., Huntington, J., Johnson, D.M., Kennedy, R., Kilic, A., Li, Z., Lymburner, L., McCorkel, J., Pahlevan, N., Scambos, T.A., Schaaf, C., Schott, J.R., Sheng, Y., Storey, J., Vermote, E., Vogelmann, J., White, J.C., Wynne, R.H., Zhu, Z., 2019. Current status of Landsat program, science, and applications. Remote Sens. Environ. 225, 127–147. https://doi.org/10.1016/j.rse.2019.02.015

Zevenbergen, L.W., Thorne, C.R., 1987. Quantitative analysis of land surface topography. Earth Surf. Process. Landf. 12, 47–56. https://doi.org/10.1002/esp.3290120107